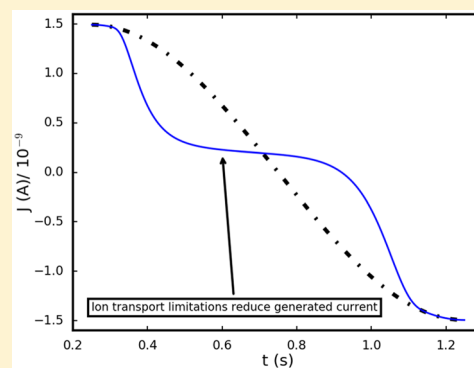


# Current-Generating Double-Layer Shoe with a Porous Sole: Ion Transport Matters

Alexei A. Kornyshev,<sup>\*,†</sup> Rebecca M. Twidale,<sup>†</sup> and Anatoly B. Kolomeisky<sup>‡</sup><sup>†</sup>Department of Chemistry, Faculty of Natural Sciences, Imperial College London (University of Science, Technology and Medicine), London, SW7 2AZ London, United Kingdom<sup>‡</sup>Department of Chemistry and Department of Chemical & Biomolecular Engineering, Center for Theoretical Biological Physics, Rice University, Houston, Texas 77005-1892, United States

**ABSTRACT:** Generating electrical current from mechanically forced variation of the contact area of electrode/electrolyte interface underpins one of the scenarios of harvesting electrical current from walking. We develop here theory of an electrical shoe with a porous sole with an account of both convection of the liquid electrolyte under pressure and ion migration with transmission-line-type charging of electrical double layer at the pore walls. We show here that ion transport limitations can dramatically reduce the generated current and power density. The developed theory describes the time dependence of the generated current and reveals its dependence on the main operation parameters, the amplitudes of oscillating pressure and frequency, in relation to the system parameters.



## INTRODUCTION

There is currently great interest in electrical current generation from mechanical motion of human individuals based on the principle of reverse electroactuation. Where direct electroactuation converts changing electric potential into mechanical motion,<sup>1,2</sup> reverse electroactuation does the opposite, usually in the form of generating transient currents, with repeated oscillating motions producing ac current.<sup>3</sup> The task here is to produce the maximum power density from the gadget at minimal degradation, i.e., maximal longevity of the device, and at low cost.

There may be different principles of reverse electroactuation that we will not review here. The one we will focus on is based on mechanical changes of the electrical capacitance of the system. When the electrical capacitance is kept under constant voltage while connected to a battery, a change in this capacitance will cause a transient current in the network, charging or discharging the capacitor. A principle such as this can also be used in tactile sensing.<sup>4</sup> The amount of current flowing in the system will be proportional to the change in capacitance, which in turn scales with its maximal value. Thus, manipulating the capacitance of a dielectric capacitor will produce much smaller currents than those using the electrochemical double-layer capacitors. Dielectric capacitance is inversely proportional to the thickness between the plates, the smallest value of which is usually not less than 100 nm, whereas electrochemical double layer capacitance is inversely proportional to the Gouy length, which depending on the concentration of electrolyte and voltage typically lies in the range of 1–10 nm.

The principle of capacitive reverse electroactuation using electrolytes has been patented by Krupenkin<sup>5</sup> and developed in the pioneering work of his group.<sup>6,7</sup> His devices are based on the compression of nonwetting electrolytic droplet(s) confined between two electrodes: When compressed, the two electrodes move closer together, and the droplet spreads and becomes wider, increasing its contact area with the electrodes, thereby increasing the capacitance. When the compression is removed, the droplets shrink back, and the contact area decreases reducing the capacitance. Since changing the capacitance at a constant voltage causes transient current, the alternation of compression and decompression will generate the alternating current patterns, and this is what Krupenkin's group demonstrated experimentally.

In a previous work,<sup>8</sup> we developed a slightly different scenario of realization of the same idea. Instead of considering a flat capacitor system, we considered a porous electrode, ordinarily nonwetted with the electrolytic solution either due to its natural solvo-/iono-phobicity or due to the Cassie–Baxter condition<sup>9</sup> of restraining of liquid penetration into a porous medium. Under sufficient external pressure, e.g., that emerging under a stepping foot, the liquid will penetrate the pores and the contact area between the electrolytic solution and the electrode will increase, thereby increasing the double layer capacitance. If the electrode is under a constant positive bias, then the electrical double layer will be rich in anions; the spreading of such a layer over the interior will produce a flow of

Received: November 11, 2016

Revised: March 1, 2017

Published: March 31, 2017

electrons away from the electrode to establish new charge equilibrium. As the electrolytic liquid recedes from the pore, the capacitance will diminish and cause a reverse flow of electrons.

Under a set of simplifying assumptions, a fully analytical theory was developed to describe the operation of such a system. Among the assumptions made, the most important ones were as follows: (1) The flow of the liquid under the varying pressure obeys the Washburn equation. (2) There is no capillary hysteresis. (3) When the liquid flows into the pore, the double layer momentarily forms at the contact surface (adiabatic approximation).

A full, detailed description of the rheology of the flow into narrow capillaries is a serious task, which must be further explored. However, for pores of 1  $\mu\text{m}$  size, the Washburn equation can be a good semiphenomenological approximation.<sup>10–13</sup> If the pore walls are ideally smooth, then hysteresis may not be essential. The role of ion transport limitations is the first thing to understand when going beyond the simple theory of the previous work.<sup>8</sup> Indeed, will the double layer charging take place momentarily with the liquid flow? If not, what will be the effect on the generated current and the average power?

The present work is intended to answer these questions by investigating a model of ion transport into the liquid that moves inside the pore. We have chosen the simplest possible model that integrates the transmission line theory of ion transport into the Washburn-like description of a pressure-induced liquid flow. This simplification allows us to develop a fully analytical theory, which will recover the result of the previous work as particular limiting case for very fast migration of ions. The resulting formulas for the time-dependent current and the average power will allow us to understand what is needed to minimize the ion migration limitations and the characteristic time related to them.

Ion transport effects in “sister problems”, such as capacitive ionization or more generally capacitive salinity gradient energy systems, have been intensively studied in a number of works, see e.g., Biesheuvel et al.,<sup>14</sup> some papers in this journal,<sup>14–17</sup> and a review article,<sup>18</sup> but to our knowledge, they have not been explored in porous reverse electroactuators.

## MODEL AND BASIC EQUATIONS

For this model, we will investigate charging of a pore using the transmission line theory in order to account for the redistribution of ions in an electrolyte not being instantaneous when following the moving liquid. We will develop the simplest version of the theory, taking into consideration that the penetration depth of the liquid into the pore,  $L(t)$ , changes with time. For this quantity we will use the form derived in the previous work,<sup>8</sup> obtained for a periodical change of external pressure and the use of Washburn equation, which describes how the liquid moves inside the pore under a variable pressure:

$$L(t) = \sqrt{\frac{2AP_0}{\omega}} \sqrt{1 - \sin(\omega t)}, t \geq \pi/2\omega \quad (1)$$

Here  $P_0$  is the amplitude and  $\omega$  is the frequency of the oscillating external pressure, e.g., emerging from walking, and  $t$  is the time over which the charging takes place. The parameter  $A$  ( $\text{m}^2 \text{Pa}^{-1} \text{s}^{-1}$ ) is defined as

$$A = \frac{r^2 + 4kr}{8\eta} \quad (2)$$

where  $r$  is the radius of the pore,  $k$  is a dimensional slip coefficient (which would have been zero for complete wetting conditions but is close to the pore radius for the nonwetting case), and  $\eta$  is the liquid viscosity.<sup>19</sup>

The expression for the evolution of charge in the pore due to the moving liquid and migration of counterions and co-ions in the flow of the liquid is obtained by incorporation of eq 1 into the transmission line equation. The transmission line theory describes the propagation of electrical current in the pore. Ideally, it works when the pore size is much larger than the thickness of the equilibrium electrical double layers at the pore walls so that one can speak about the ion transport in the “bulk” of the pore charging the double layer capacitor at the walls. Eventually, it will work even for narrow pores, but only if the electrical double layers on opposite sides of the pore do not overlap.

In the transmission line theory, the ionic current along the pore axis is not conserved as it gets converted into the capacitor's charge along the surface; in this respect, the electrode surface works as a “sink” of capacitive current. The transmission line model has been explored and exploited from the beginning of the 20th century (for review, see one of the latest papers utilizing it).<sup>14</sup> Similar types of equations have emerged and been studied, not only in electrical engineering and electrochemistry but also in one-dimensional heat transfer.<sup>20</sup> In the capacitive charging of a capillary of fixed length  $L$  completely filled with an electrolyte taking place after a voltage jump  $\bar{u}$ , the equations of the transmission line theory give the following formula for the evolution of the net charge in the pore (for derivation, see Appendix A).

$$Q(t) = \bar{u}C_0l_pL \frac{2}{\pi^2} \sum_{n=0}^{\infty} \frac{1}{\left(n + \frac{1}{2}\right)^2} \left\{ 1 - e^{-\left(n + \frac{1}{2}\right)^2 \pi^2 \frac{l_p^2}{L^2} \cdot t} \right\} \quad (3)$$

Here,  $\bar{u}$  is the potential difference between the electrode (pore surface) and the bulk electrolyte,  $C_0$  is the double layer capacitance per unit surface area of the pore (considered to be voltage independent),  $l_p$  is the average pore perimeter, and  $1/l$  is the specific surface area of the pore, i.e.,  $1/l = S/V$  where  $S$  is the surface area of the pore and  $V$  is the volume of the pore. For cylindrical pores, we have  $l_p = 2\pi r$  and  $l = r/2$ ; therefore,  $l_p = 4\pi l$ . This relationship is used throughout this work when calculating the values of parameters used in the graphs.

The following combination of parameters determines here the quantity of the dimensionality of time.

$$\tau = \frac{C_0l}{\Sigma} \quad (4)$$

where  $\Sigma$  is the ionic conductivity of the electrolytic solution that we use to fill the pore. This time increases with poorer conductivity of the electrolyte because the ions will be migrating slower to reach the areas they need to charge and as the double layer capacitance becomes larger because for a given voltage more charge will need to be transported to those areas. However, in a transmission line system the relaxation time is much longer than  $\tau$ ; it is, actually, equal to

$$\tau_p = \frac{1}{\pi^2} \frac{L^2}{l^2} \tau \quad (5)$$

This time increases with the length of the filled pore, as  $L^2$ , and decreases with increasing pore cross section.

Note that eq 3 is valid under the assumption that  $C_0$  does not depend on applied voltage. This is generally never the case in electrochemistry, but this approximation allows us to obtain analytical results; furthermore, the effect of voltage dependence often averages out in the whole sample when considering pore size distribution.<sup>21</sup>

In our case, however, we are not considering a voltage jump. On the contrary, the electrode potential relative to the bulk electrolyte (reference electrode) is kept constant, and it is now the depth of the liquid penetration into the pore which changes. However, all the boundary conditions are the same. If we assume that the speed of migration of ions is faster than the convection of the liquid, then we can suggest the next level of the “adiabatic” approximation by substitution of eq 1 for  $L(t)$  into the transmission line equation (eq 3). By using this crude approximation, we decouple the problems of convection and migration but incorporate them in one process. We critically analyze it in the end of this section. Once adopting it, we obtain a formula for the evolution of the net charge in the pore over one period of oscillation of external pressure

$$Q(t) = \bar{u} C_0 l_p \sqrt{\frac{2AP_0}{\omega}} \sqrt{1 - \sin(\omega t)} \left\{ 1 - e^{-\left(n + \frac{1}{2}\right)^2 \pi^2 l^2 / \left[ \frac{2AP_0}{\omega} (1 - \sin(\omega t)) \frac{t}{\tau} \right]} \right\}, \pi / 2\omega \leq t \leq 5\pi / 2\omega \quad (6)$$

This equation describes the charge within each period. At the onset point of each period there is no liquid in the pore,  $L = 0$ , and this is the same at the end of the period. One of the main assumptions here is that when the liquid returns from the pore to the bulk there is no memory in the system: counterions do not crowd up at the entrance of the pore. Thus, hereafter, we will be considering only one period of pressure oscillation, assuming that once the electrolyte has been pushed out of the pore to its original position there will be no “memory” of the previous period. The electrolyte will act in exactly the same way every single time it enters the pore.

Looking at eq 6, we see that the characteristic time to charge the pore over the maximum penetration length for a given amplitude of pressure is not  $\tau$ , as we have already commented above, but something close to

$$\tau_p = \frac{8AP_0}{\pi^2 l^2 \omega} \tau \quad (7)$$

How large could this time be? Taking  $\Sigma = 0.14$  S/m for 0.1 molar aqueous solution of KCl,  $l = 5 \times 10^{-7}$  m, and  $C_0 = 0.1$  F/m<sup>2</sup>, we get  $\tau = 3.6 \times 10^{-7}$  s. With  $A = 10^{-10}$  m<sup>2</sup> Pa<sup>-1</sup> s<sup>-1</sup> and  $P_0 = 10^5$  Pa, this gives  $\tau_p = 1.9$  s, which is longer than the 1 s period of oscillation. For 1 M electrolyte, the conductivity will be 10 times larger, and  $\tau$  and  $\tau_p$  will be 10 times shorter. In that case, our adiabatic approximation would be rigorous, but then the effect of ion migration limitations will be small. However, there is in fact no simple relaxation time behavior in eq 6, because of the factor  $1 - \sin(\omega t)$  in the denominator of the exponent. At certain sections of a period when  $\sin(\omega t)$  is close to 1, the response is much faster. Furthermore, due to the series structure of the result, the time dependence at small times is not exponential but rather proportional to  $\sqrt{t}$  (c.f. Appendix A). Thus, extending the theory to the case when  $\tau_p$  is on the order of the period of pressure oscillation has a character of

extrapolation, which as we will see below seems to give physically reasonable results. With these reservations in mind, let us now explore the consequences of eq 6.

## RESULTS AND DISCUSSION

**Charge Evolution.** In Figure 1, using a set of estimated realistic values for the parameters listed in the caption, we show

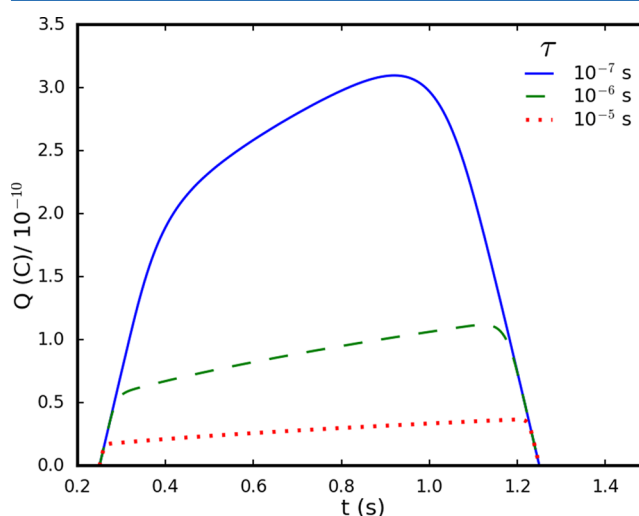


**Figure 1.** Charge accumulated in a solvophobic pore over a period of application of periodically varying external pressure: effect of ion transport limitations. Different curves correspond to different values of the intrinsic migration times  $\tau$ . The slower the characteristic migration time  $\tau$  (see text), the less charge will have time to accumulate in the pore. The values for the parameters used in this plot are  $\bar{u} = 0.3$  V,  $C_0 = 0.1$  F m<sup>-2</sup>,  $l = 0.5 \cdot 10^{-6}$  m,  $A = 10^{-10}$  m<sup>2</sup> Pa<sup>-1</sup> s<sup>-1</sup>,  $P_0 = 10^5$  Pa, and  $\omega = 2\pi$  s<sup>-1</sup>. The effect of the characteristic migration time on charge accumulation in the pore is investigated here over three different orders of magnitude.

the evolution of charge within one pore over a 1 s period of pressure oscillation for indicated values of the intrinsic migration times.

There are three regimes in the dynamics of the charge accumulation as shown in Figure 1. The amount of charge initially increases linearly, the accumulation rate then changes to produce a shallower gradient, and finally it starts to linearly decrease. From eq 6, it can be shown that for times close to  $\pi/2\omega$  we have in the first regime  $Q(t) \approx C_0 l_p \sqrt{AP_0 \omega} \left( t - \frac{\pi}{2\omega} \right)$ , while in the third regime closer to  $5\pi/2\omega$ ,  $Q(t) \approx C_0 l_p \sqrt{AP_0 \omega} \left( \frac{5\pi}{2\omega} - t \right)$ . The charge evolution in the middle regime is different and is already affected by the migration time.

This behavior is nontrivial, but is still easy to rationalize. At the beginning and the end of the period, the charging-discharging dynamics is independent of the ion migration because in these cases the rate-limiting is the motion of the liquid as a whole. It is only in the middle region, when the ion migration cannot follow the liquid filling or leaving the pore, that the diffusion of ions becomes a rate-limiting step. Therefore, the faster the ion migration, the shorter the duration of this intermediate regime. In other words, as the liquid enters the pore, the ions immediately follow it because the speed of the liquid motion in the pore is initially low, as well as the penetration depth being small. Later, however, the speed of

pore filling accelerates, and the depth increases. At the central point of the period ( $t = \frac{3\pi}{2\omega}$ ), the penetration depth reaches its maximum and begins to return to the opening. The peak of the graph is the point at which the flow of counterions meets the returning liquid front, and the liquid and the ions together return to the bulk liquid outside the pore.

The migration time,  $\tau$ , is short and, depending on the conductivity of the electrolyte and the double layer capacitance per unit surface area, lies in the range of  $10^{-7}$ – $10^{-5}$  s. The characteristic time to charge the pore,  $\tau_p$ , over the maximum penetration length, however, is much longer. For a set of typical parameter values,  $l = 0.5 \times 10^{-6}$  m,  $A = 10^{-10}$  m<sup>2</sup> Pa<sup>-1</sup> s<sup>-1</sup>,  $P_0 = 10^5$  Pa,  $\omega = 2\pi$  s<sup>-1</sup>, and  $\tau = 10^{-6}$  s, eq 7 gives us  $\tau_p = 1.29$  s. Such a value is close to the pressure oscillation period (1 s); hence, we should see a delay in “charge delivery” into the pore sensitive to the values of parameters – the exact value of  $\tau$  in the first place. By changing the order of magnitude of  $\tau$ , we can see what will be the effect of the delayed migration of ions. When comparing the characteristic time,  $\tau_p$ , for the three different values of  $\tau$  used in the plots above, we obtain  $\tau_p = 0.129$ , 1.29, and 12.9 s when  $\tau = 10^{-7}$ ,  $10^{-6}$ , and  $10^{-5}$  s, respectively. From these values and applying them to eq 6, we can deduce that as the characteristic time,  $\tau$ , becomes quicker, the exponential term vanishes much faster, bringing the result much closer to that of the adiabatic approximation with no lag in the migration current. This makes sense, as the quicker the ions migrate and form the double layer inside the pore, the faster the current will be generated and the smaller the lag in the current.

**Generated Current.** The net current of ions is just time derivative of the charge

$$J(t) = \frac{dQ(t)}{dt} \quad (8)$$

It will be equal and opposite in sign to the electronic current in the electrode to meet the ions, but since the current in electrical engineering is defined as the flow of positive charges, eq 2 gives us the current in the network. Note again that the ion current is not constant along the pore; it “sinks”, charging the pore walls. By definition the ionic current must be zero at the front of the liquid moving in the pore, as no ion can cross this front. Differentiation of eq 4 gives the time dependence of the net ionic current inside a single pore

$$J(t) = \frac{\bar{u}C_0l_pI^2}{\tau} \sqrt{\frac{2\omega}{AP_0}} \left\{ \frac{-\sin(\omega t) + \omega t \cos(\omega t) + 1}{(1 - \sin(\omega t))^2} \right. \\ \left. \sqrt{1 - \sin(\omega t)} \sum_{n=0}^{\infty} e^{-(n+\frac{1}{2})^2 \pi^2 l^2 / \left[ \frac{2AP_0}{\omega} (1 - \sin(\omega t)) \frac{t}{\tau} \right]} \right. \\ \left. - \frac{2\bar{u}C_0l_p}{\pi^2} \sqrt{\frac{\omega AP_0}{2}} \frac{\cos(\omega t)}{\sqrt{(1 - \sin(\omega t))}} \sum_{n=0}^{\infty} \frac{1}{\left(n + \frac{1}{2}\right)^2} \right. \\ \left. \left\{ 1 - e^{-(n+\frac{1}{2})^2 \pi^2 l^2 / \left[ \frac{2AP_0}{\omega} (1 - \sin(\omega t)) \frac{t}{\tau} \right]} \right\} \right\}, \\ \pi/2\omega \leq t \leq 5\pi/2\omega \quad (9)$$

with all parameters having the same definition as those in eq 6.

Figure 2 plots this current for three values of the intrinsic migration time,  $\tau$ , the same as those used in the plots for the charge evolution in Figure 1, plus one more curve, plotted for a

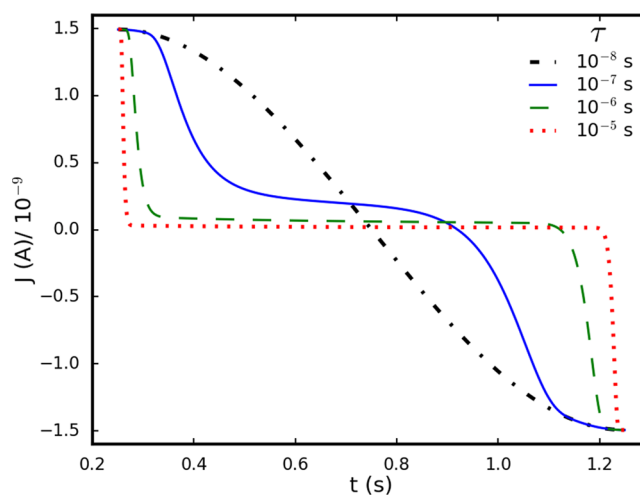


**Figure 2.** Absolute current generated in a single solvophobic pore over a period of application of periodically varying external pressure. As in Figure 1, the slower the intrinsic migration time  $\tau$  (see the text), the less time the charge has to accumulate in the pore, so less current will be generated per period. Therefore, for a slower characteristic time, the plot produced a more prominent lag in the current. The values for the parameters used in this plot are the same as those used in Figure 1. The effect of the characteristic migration time on current generation in the pore is investigated here over four different orders of magnitude, recovering the result of the previous work<sup>8</sup> only when the migration time reached is unphysically small ( $10^{-8}$  s).

very short migration time (unphysically short), to check whether we could recover the fully adiabatic regime limit.<sup>8</sup> Similar to the charge dynamics, there are three regimes for the current. At the beginning of the period, the current is constant and is equal to  $J = C_0l_p\sqrt{AP_0\omega}$ , while at the end of the period it has the same magnitude but opposite sign.

As we see from Figure 2, changing the intrinsic migration time  $\tau$  will change the way the charge evolves and therefore change the amount of current the electrode will produce over one period. As  $\tau$  increases, the current is generated only at the beginning and the end of the period, remaining very small in the middle. As  $\tau$  decreases, current generation is more even; in this process, ions with almost no delay charge the length of the pore penetrated by the liquid. When the order of magnitude of  $\tau$  becomes as small as  $10^{-8}$ , the plot does not show any delay, essentially reproducing the result obtained in the previous work under the adiabatic regime.<sup>8</sup>

**Power.** Calculation of the power that an electromechanical capacitive current generator can produce is a special task which requires consideration of particular circuit which may generally contain resistive, inductive, and capacitive elements. The combination of these elements will affect the value and time dependence of the generated current, as well as the power pumped into the load. We consider nothing of the kind in this paper, but in Appendix C, we investigate the conditions under which we can calculate the capacitively generated current neglecting the load. Thus, when speaking below about the “power” we will estimate the maximum amount of electrical energy that our variable capacitor can produce over half-a-period of pressure oscillation in a “short-cut” circuit. Hereafter, we will designate it as “short-circuit” power density, and when the adjective is omitted for brevity, we still mean such quantity. It benchmarks the general capability of device, the implementation of which must generally be studied with the

consideration of the full circuit (for details, see Appendix C). For such a defined quantity, we can obtain a simple analytical expression.

This can be calculated as

$$W = \langle J \rangle \bar{u} \quad (10)$$

where the average current density  $J$  is defined as characteristic current per unit surface area of the sole of the shoe, averaged over a half of a period (because two halves of the period are symmetric).

$$\langle J \rangle = \frac{\varepsilon}{\pi r^2} \frac{\omega}{\pi} \int_{\pi/2\omega}^{3\pi/2\omega} J(t) dt \quad (11)$$

Here,  $\varepsilon$  is the porosity of the sole of the shoe and  $r$  is the radius of a single pore (we mean the average radius). Recalling eq 8, we can remove the integral in eq 11 to obtain

$$\langle J \rangle = \frac{\varepsilon}{\pi r^2} \frac{\omega}{\pi} \left[ Q\left(\frac{3\pi}{2\omega}\right) - Q\left(\frac{\pi}{2\omega}\right) \right] \quad (12)$$

Substituting eq 6 into eq 12 and taking into account that  $\frac{2}{\pi^2} \sum_{n=0}^{\infty} \left(n + \frac{1}{2}\right)^{-2} = 1$ , we finally obtain a compact expression for the power density per unit area of the sole

$$W = \varepsilon \frac{2}{\pi l} C_0 \bar{u}^2 \sqrt{AP_0 \omega} \left( 1 - f\left(\frac{3l^2}{8AP_0 \tau}\right) \right) \quad (13)$$

where the function  $f(x)$  is defined as

$$f(x) = \frac{2}{\pi^2} \sum_{n=0}^{\infty} \frac{1}{\left(n + \frac{1}{2}\right)^2} e^{-\left(n + \frac{1}{2}\right)^2 \pi^2 x} \quad (14)$$

Without the second term in the brackets, eq 13 would give the same result as in the fully adiabatic theory of the previous work<sup>8</sup> (see eq 17 of ref 8, with  $r$  there replaced by  $2l$ , with account to the correction to this equation).<sup>22</sup> Thus, it is the  $f$  term that reduces the power density. Of course, when  $\tau \rightarrow 0$ , then  $x \rightarrow \infty$  and  $f \rightarrow 0$ , and the result of the fully adiabatic theory<sup>8,22</sup> is recovered. Otherwise, the  $f$  term may comprise a substantial reduction of the power density. Since  $f(x)$  is a universal function and not dependent on any other parameters, it is worth displaying (Figure 3).

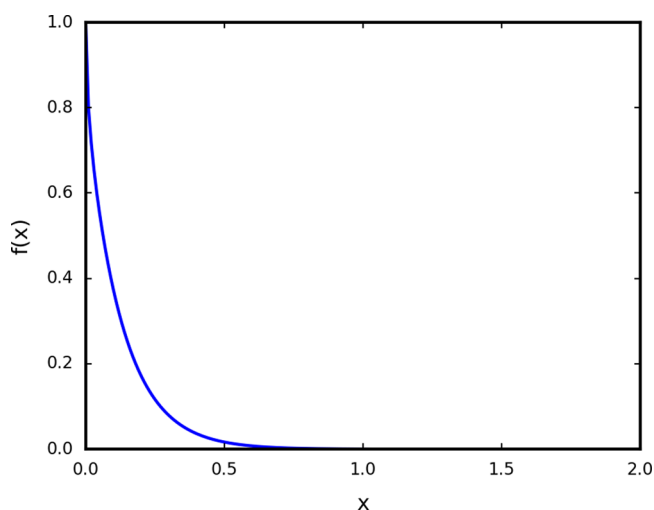


Figure 3. Graph of  $f$  function defined by eq 12.

For a typical set of parameters,  $l = 0.5 \times 10^{-6}$  m,  $A = 10^{-10}$  m<sup>2</sup> Pa<sup>-1</sup> s<sup>-1</sup>,  $P_0 = 10^5$  Pa,  $\tau = 10^{-6}$  s, and  $x = \frac{3l^2}{8AP_0\tau} = 9.375 \times 10^{-3}$ , eq 14 gives  $f = 0.806$  so that due to the lag in the “ion response” more than 80% of the power would be lost compared to the fully adiabatic “ideal world”.<sup>8,22</sup> However, if the migration time is 1 order of magnitude shorter, then the same estimate will give  $f = 0.392$ , i.e., only 39.2% of power is lost due to ion migration limitations. On the contrary, if migration time is estimated to be 10 times longer,  $f = 0.939$ , the system will function at only 6% of its ideal efficiency. We show the graph of the power (Figure 4), for the same set of parameters, showing its dependence on  $\tau$ .

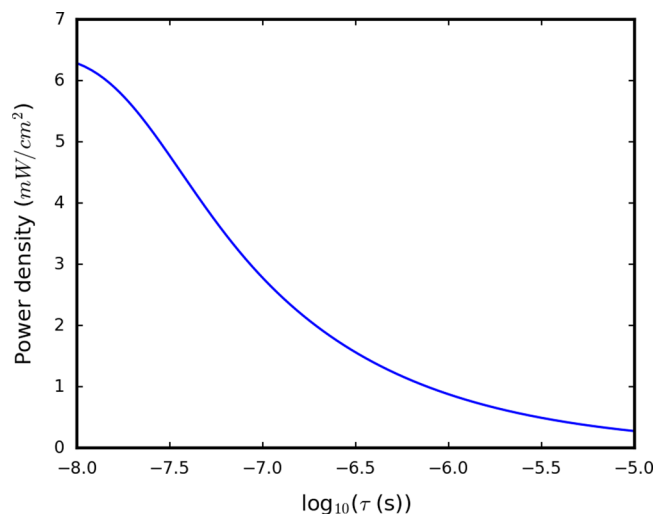
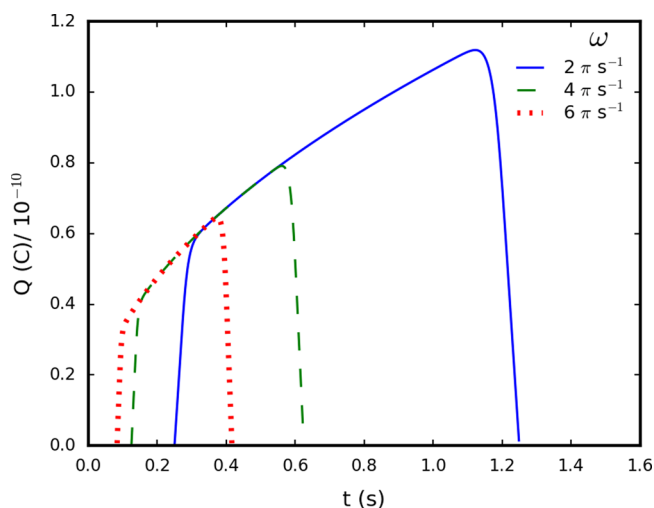


Figure 4. Generated power for the charging of hydrophobic pores, changing the intrinsic migration time of ions in the electrolyte, plotted using eq 13. At very short ion migration times, the generated power density increases slowly with decreasing migration time. However, as the migration time becomes longer, the power density decreases much faster, tending toward a much lower power density. The parameters used in this plot are the same as those in Figure 1, with  $\varepsilon = 0.5$ . The characteristic migration time,  $\tau$ , is changed logarithmically to view the full effect on the power density.

In accordance with the above-discussed analysis of the  $f$  factor, Figure 4 shows that there is a point around  $\tau = 10^{-7}$  where power density increases at a slower rate with decrease of the rate of migration. This is because for the taken set of parameters the ions are reaching the value of  $\tau$  where they have time to reach even the peripheral parts of the liquid in the pore while the liquid moves there; the plot looks as though it will reach a saturation point if the migration time is decreased even further. We can see, however, that the general trend is that as the migration time increases the average current output over the soles decreases and so does the power density.

**Changing the Period of Oscillation at Constant Migration Time.** So far we have kept all parameters constant aside from the characteristic migration time,  $\tau$ . Now we will investigate the effects of changing the period of walking,  $\omega$ , while keeping the migration time at a constant value of  $10^{-6}$  s. Realistically, a rate of 1 step per second is a slow walk, so we will consider what happens to the generated power density when we increase the speed, or decrease the length of the period, to 2 steps per second;  $\omega = 4\pi$  s<sup>-1</sup> (a fast walk); and 3 steps per second;  $\omega = 6\pi$  s<sup>-1</sup> (a fast run). In Figures 5 and 6,

respectively, we show the effect that the frequency has on the evolution of charge in the pore and the generated current



**Figure 5.** Charge accumulated in a solvophobic pore over one period of application of a periodically varying external pressure. The plot shows the effect of frequency of the applied pressure on the charge accumulated in the pore. As the frequency increases from  $\omega = 2\pi \text{ s}^{-1}$  to  $\omega = 6\pi \text{ s}^{-1}$ , the total amount of charge generated at the pore decreases. This is because as the frequency increases the liquid spends less time in the pore, so the ions have less time to form the double layer inside the pore. The parameters have the same values of those used to plot Figure 1, aside from  $\tau$  being fixed at  $10^{-6} \text{ s}$  and  $\omega$  being set as shown in the inset.

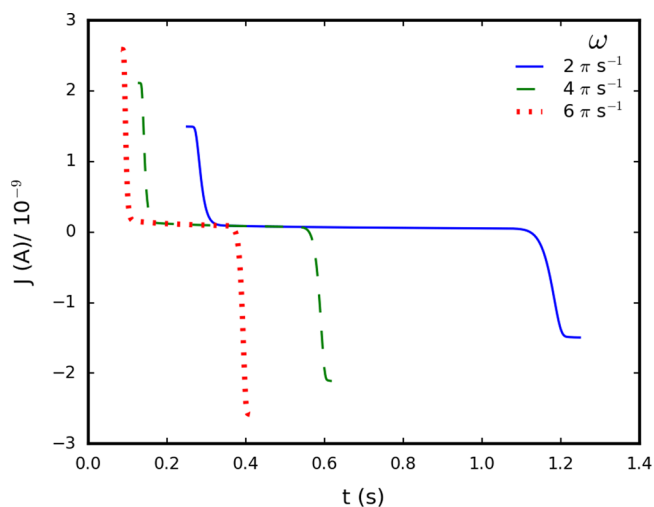


**Figure 6.** Absolute current generated in a single solvophobic pore over one period of application of periodically varying external pressure. This plot shows the effect of the frequency of the applied pressure on the generated current. The parameters used are the same as those in Figure 1, aside from  $\tau$  being fixed at  $10^{-6} \text{ s}$  and different values of  $\omega$  being set between  $2\pi \text{ s}^{-1}$  and  $6\pi \text{ s}^{-1}$ , as shown in the inset.

In Figure 5, we can see that changing the frequency does not change the shape of the plot qualitatively, but it affects it quantitatively. Of course, the period of a single step,  $T$ , decreases as frequency,  $\omega$ , increases:  $T = \frac{2\pi}{\omega}$ . Thus, as the period decreases, the plots become narrower. The initial gradients increase, which indicates that speed of charge generation increases with decreasing time period, even if the

overall amount of charge generated decreases. This is due to the speed of the oscillating pressure increasing with decreasing period so that the liquid enters the pore much faster, but it doesn't have enough time to go deep into the pore. To recharge the double layers, the ions have to migrate shorter distances, and the lag effect is less felt. This is supported by the trends in the current shown in Figure 6. As the period gets shorter, the initial current generated at the pore becomes larger.

The combined effect of the frequency and period on the power density generated in the pore is simple. Following eq 13, it scales  $\propto \sqrt{\omega}$ , in the same way as it does in the fully adiabatic case,<sup>8,22</sup> but due to the migration delay, the proportionality factor is smaller. However, again, we can see that the faster you walk the greater the amount of the generated power. This trend is shown in Figure 7.

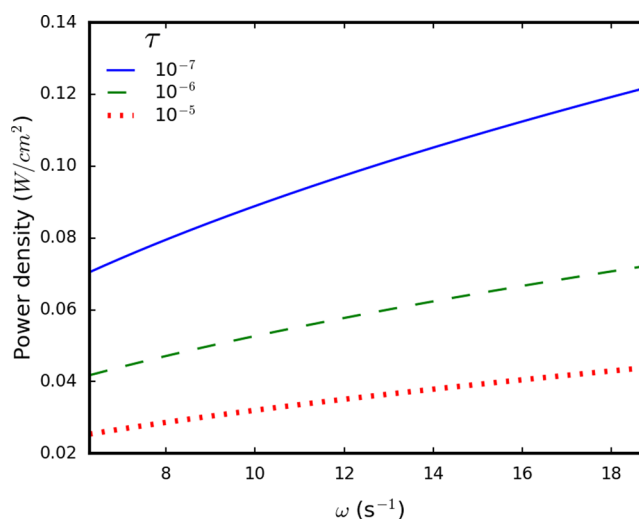


**Figure 7.** Short-circuit power density generated with changing frequency of oscillating pressure, shown for three different migration times. The power generated increases with the square root of frequency, described by the simple power law of eq 13. As migration time decreases, the power increases. The parameters used in this plot are the same as those in Figure 1, aside from  $\omega$  now continuously varying between  $2\pi$  and  $6\pi \text{ s}^{-1}$  and  $\varepsilon = 0.5$ .

Decreasing the size of the pores allows a larger amount of current to be generated due to the increase in the number of pores on the sole per unit cross-sectional area; therefore, the system will operate with larger overall surface area available for charging. Charging of all pores will proceed in “parallel” so that that the increase of the area in this way will not slow down charging.

**Pressure Dependence.** Here the  $f$  term brings a dramatic effect. The behavior of the power with the increase of pressure is determined by the behavior of the function  $1 - f(x)$ . Indeed, there is an asymptotic law for this function: As  $x \rightarrow 0$ ,  $1 - f(x) \approx 2\sqrt{x}$ , but the factor in front of  $1 - f(x)$  in eq 13 is  $\propto \frac{1}{\sqrt{x}}$ .

Thus, as  $x \rightarrow 0$ ,  $\frac{1-f(x)}{\sqrt{x}} \approx 2$ . With increasing  $P_0$ ,  $x \rightarrow 0$ , and the power increases. However, it then saturates to a constant value. This value is given by a simple formula:

$$W = 0.78\varepsilon C_0 \bar{U}^2 \sqrt{\frac{\omega}{\tau}} \quad (\text{high pressure limit}) \quad (15)$$

Of course when pressure goes to zero,  $f(x) \approx 0$ , and  $1 - f(x) \rightarrow 1$ . Thus

$$W = \varepsilon \frac{2}{\pi l} C_0 \bar{U}^2 \sqrt{AP_0 \omega} \quad (\text{low pressure behaviour}) \quad (16)$$

(which is the result of the previous work<sup>8</sup> with account for correction of the numerical coefficient).<sup>22</sup>

Thus, the power increases initially as the square root of pressure amplitude and then saturates at the maximally possible limiting value. This limitation holds because increasing pressure amplitude decreases the time that liquid spends in the pore, and there is no time for redistribution of ions to take place. Figure 8

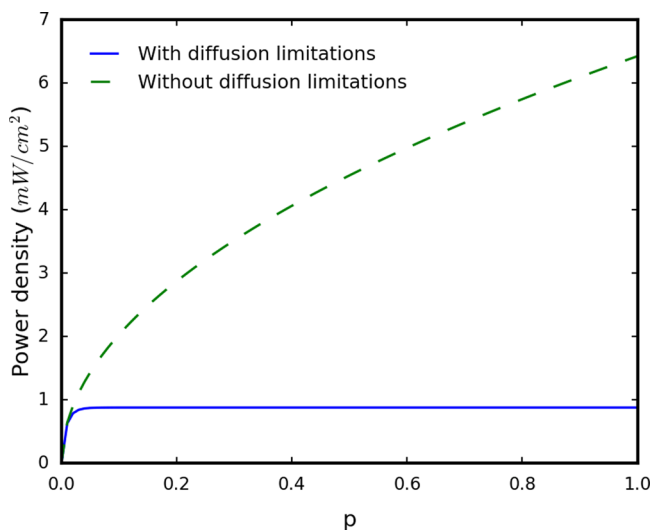


**Figure 8.** Pressure dependence of the short circuit power density, as a function of  $p$ , the portion of pressure of  $10^5$  Pa. (For an average adult individual,  $p \sim 1$ ). The blue solid curve is calculated via eq 13. Parameters are the same as those in Figure 1, and  $\varepsilon = 0.5$ . For comparison, the dotted green curve corresponds to the case of no diffusion limitations (eq 16).

shows the full graph of the pressure dependence. For typical estimates that we used in this paper, a walking individual is already at the plateau in terms of the pressure dependence due to migration limitations. However, a child will produce less than that (for them, the migration limitations will be less important).

Our theoretical calculations have been done for the case when the pressure changes periodically as  $\sim \sin(\omega t)$ , but the analysis can be extended to more general variations in pressure. Such calculations for the pulsed staircase variations are presented in Appendix B. It is found that all qualitative results obtained above are confirmed, and only the amplitude of properties are slightly modified.

## CONCLUDING REMARKS

Let us summarize what we have done and learned, what we think we know, and what we yet do not know. Using a simple combination of the Washburn equation and the transmission line theory, we obtained a close form formulas describing the operation of a machine based on pressing electrolytic liquid into pores of a polarized electrode.

We would have had to develop a more complicated theory, involving the Nernst–Planck equation,<sup>23</sup> if the drag coefficients for cations and anions, i.e., how they are drawn in a forced convective flow, were different. If however they are roughly the same, then convection itself will not affect the flow of net charge. This allowed us to consider the charging migration current as being driven exclusively by the electrical potential

and independent of convection but proceeding in a liquid column of varying length. We considered the principle issues of this process and thus studied effects in one single pore, extending it later on a monodisperse system of parallel pores.

Integration of our findings into the theory of electrodes with pore size distribution and complex shapes of the pores was beyond our goals; such investigation may have multifarious aspects and will be the subject of future studies. However, modern technology can build at least laboratory prototypes in which the electrode may have a system of monodisperse cylindrical pores with an ideal internal surface so that the results of our findings can be tested experimentally as they are.

Using the chosen theoretical model, we have found that the ion migration limitations may have a serious impact on generated power. It affects the slope of the frequency dependence of generated power, which as a function of frequency should obey the  $\omega^{1/2}$  law. It levels off its pressure dependence; with the increase of the amplitude of the oscillating pressure, the power first increases square root wise,  $\propto P_0^{1/2}$ , but then reaches saturation. The latter takes place only when the ion migration limitations are taken into account.

We should recall that the simple combination of two theories seems physically justified when the characteristic time  $\tau_p$  (eq 7) is not much greater than the oscillation period  $T = 2\pi/\omega$ . Eventually with the increase of frequency,  $\tau_p$ , which is  $\propto 1/\omega$ , decreases with the same rate; thus, the  $\omega^{1/2}$  law is, perhaps, not limited by the approximations of the theory.

We are less sure about the pressure dependence law. If the criterion is indeed  $\frac{2AP_0}{\pi^2 l^2 \omega} \tau < \frac{2\pi}{\omega}$ , i.e.,  $\tau < \frac{\pi^3 l^2}{4AP_0}$ , then we are already at the border of applicability of the theory. Our “typical estimate” suggests that  $\tau < \frac{\pi^3 10^{-12}}{10^{-10} \times 10^5} \approx 3 \times 10^{-6}$  s, which more or less holds already for  $\tau = 10^{-6}$  s, and is warranted for shorter values of  $\tau$ . It will get worse with further increase of pressure.

Building a fully consistent theory strictly applicable in all limiting cases is a challenging future task. However, although the common sense advises us that we must maintain certain elements of “adiabaticity” when “constructing” the combination of two theories, the results that we have obtained look meaningful in all the studied limits. We thus leave it for experiments to test the predictions of this simple theory. Discrepancies with it will motivate development of more complicated approaches.

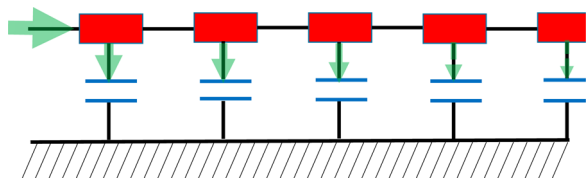
As already mentioned, nowhere in the paper have we considered the effect of the load on the resulting current and power. Indeed, the voltage drop across the capacitor must generally be affected by other elements of the full circuit and would depend on the Ohmic potential drop across the load, which in turn depends on the current. Equations of the current then become generally much more complicated (for the Ohmic drop and simple sinusoidal signals they can be obtained in analytical form, as shown by Krupenkin and Taylor).<sup>6</sup> In Appendix C, we derive a criterion, when the effect of a resistive load on the equations for the current and power generation can be neglected, analyzing its consequences for the case of “walking frequencies” and estimated capacitances. The corresponding constraints could be even more serious, if we used Krupenkin’s patched surfaces that dramatically increase the frequency of the current oscillation. Such other options may be considered in future developments of the double-layer shoe with ultraporous soles based on, for example, the structures of

functionalized carbon nanomaterials. Consideration of full circuits is a subject of electrical engineering, which is beyond the scope of a paper devoted to physical-chemical aspects of the electrical double-layer-based capacitive power generation, but in laboratory experiments aimed on testing predictions of this theory, the conditions specified in Appendix C should be obeyed.

The ambition to build structures with narrow pores to increase the surface area and the current may encounter completely different problems, related to capillary hysteresis,<sup>24</sup> full stall of the liquid in the pore, and a number of other side effects, as discussed in previous work.<sup>8</sup> Thus, the theory presented here tells us what fundamental limitations we could face already in the “ideal world”, based on essential physics that cannot be bypassed by mere improvement of the quality of solid surfaces.

## APPENDIX A: TRANSMISSION LINE CHARGING

The transmission line theory has existed for, perhaps, over a century and can be applied in different contexts.<sup>25</sup> As we could not find in the literature the solution obtained in the format exactly needed for this paper, we briefly outline here the principles of its derivation and the properties of the result, which also makes it easier to understand approximations made in the main text.



The sketch of the transmission line is described here. The electrical current, which in our context is the current of ions through the electrolyte, runs along a set of resistors. Current is blocked at the end point of the line, but on its propagation, it can charge a chain of capacitors. There can be no stationary current across such system, only a transient one, triggered by jump-wise change of voltage. We will consider below such a situation (in the main text we readjust it to the case of a constantly applied voltage and changing length of the line). De Levie was, presumably, the first to apply such model for calculation of impedance of charging porous electrodes filled with electrolyte.<sup>26</sup> Very recently, it has been used in the problem of capacitive desalination.<sup>14</sup>

### Basic Equations

In the continuum version of the theory, we first have the continuity equation

$$\frac{\partial J(z, t)}{\partial z} = -j(z, t) \quad (\text{A.1})$$

Here,  $z$  is the coordinate along the pore,  $t$  is time,  $J$  is the ionic current density,  $j$  is the sink current that charge the capacitance of the double layer at the interface, where

$$j(z, t) = \frac{\partial q(z, t)}{\partial t} \quad (\text{A.2})$$

and  $q(z, t)$  is volume charge density in the double layer at the wall of the pore. The latter can be expressed through the surface charge density,  $\sigma(z, t)$

$$q(z, t) = \sigma(z, t) \frac{S}{V} \quad (\text{A.3})$$

where  $S$  is the internal surface area of the pore and  $V$  is its volume. Thus,

$$\frac{S}{V} = \frac{1}{l} \quad (\text{A.4})$$

where  $l$  is the characteristic size of the pore. For a cylindrical pore of radius  $r$ ,  $l = \frac{\pi r^2 L}{2\pi r L}$  where  $L$  is the length of the pore, so that

$$l = r/2 \quad (\text{A.5})$$

Let us now introduce the potential in the “bulk” of the pore,  $\varphi(z, t)$ . The double-layer capacitance per unit surface area as a function of a potential drop across the double layer,  $(\varphi_{\text{electrode}} - \varphi)$ , is defined as

$$C(\varphi_{\text{electrode}} - \varphi) = \frac{\partial \sigma_{\text{electrode}}}{\partial (\varphi_{\text{electrode}} - \varphi)} = \frac{\partial \sigma}{\partial (\varphi - \varphi_{\text{electrode}})} \quad (\text{A.6})$$

Combining eqs A.6, A.3, and A.2, we obtain

$$\frac{\partial q}{\partial t} = -\frac{1}{l} C(\varphi_{\text{electrode}} - \varphi) \frac{\partial (\varphi_{\text{electrode}} - \varphi)}{\partial t} \quad (\text{A.7})$$

We can substitute this into eqs A.2 and A.1 to obtain

$$\frac{\partial J(z, t)}{\partial z} = \frac{1}{l} C(\varphi_{\text{electrode}} - \varphi) \frac{\partial (\varphi_{\text{electrode}} - \varphi)}{\partial t} \quad (\text{A.8})$$

We must also take into account Ohm’s law

$$J = -\Sigma \frac{\partial \varphi}{\partial z} \quad (\text{A.9})$$

where  $\Sigma$  is the ionic conductivity.

Using the notation for the potential drop across the double layer

$$u(z, t) = \varphi_{\text{electrode}}(t) - \varphi(z, t) \quad (\text{A.10})$$

and combining eqs A.9 and A.10, we obtain the master equation:

$$\frac{\partial^2 u}{\partial z^2} = \frac{C_0}{l\Sigma} \Psi(u) \frac{\partial u}{\partial t} \quad (\text{A.11})$$

where we have introduced the following convenient notations:

$$\Psi(u) = C(u)/C_0 \quad (\text{A.12})$$

Here  $C_0 = C(u = 0)$  is a linear response capacitance, and  $\Psi(u)$  is a function describing how the real capacitance of the double layer changes with voltage across the double layer. If it does not change with voltage (almost never the case!), then  $\Psi(u) = 1$ . Note that  $C_0 = C(u = 0)$ . Hereafter, we proceed assuming  $\Psi(u) = 1$ , as only in this case can one obtain transparent analytical results. With  $\Psi(u) = 1$ , eq A.11 becomes a familiar “diffusion-type” equation.

We consider the following initial and boundary conditions. At the initial time moment, the pore is completely electro-neutral all the way along.

$$u(z, t = -0) = 0 \quad (\text{A.13})$$

This changes jump-wise. At the entrance of the pore, the potential is assumed to be momentarily screened and equal to the potential drop between the electrode and the bulk of the solution, which we call  $\bar{u}$ ; therefore,



$$u(0, t > 0) = \bar{u} \quad (\text{A.14})$$

This is because there are many ions at the pore entrance, so the counter electrode is close. They do not need to migrate a long distance to the double layer at the entrance. Finally

$$\left. \frac{\partial u(z, t)}{\partial z} \right|_{z=L} = 0 \quad (\text{A.15})$$

The latter condition is understood using the Coulomb law: It states that the current at the closed end of the pore (if it has closed end) or in the middle of the pore (if its both ends are open) is zero. Depending on the situation,  $L$  will stand either for the length of the pore or half length of the pore (we of course have already assumed in all the corresponding equations above that the pore structure and properties do not change along its length). In the context of the present paper,  $L$  will stand for the length of the liquid column penetrating into the pore, because ions of electrolyte redistribute within the liquid phase not shooting into the gas phase.

### The Solution

To make our equations more compact, let us use dimensionless notations:

$$\tau = C_0 l / \Sigma, Z = z/l, S = t/\tau, \Lambda = L/l \quad (\text{A.16})$$

and

$$U = \frac{eu}{k_B T}, \bar{U} = \frac{e\bar{u}}{k_B T} \quad (\text{A.17})$$

Our master equation will then take a “parameter-free form”

$$\frac{\partial^2 U}{\partial Z^2} = \frac{\partial U}{\partial S} \quad (\text{A.18})$$

with the conditions

$$U(Z, S = -0) = 0 \quad (\text{A.19})$$

$$\left. \frac{\partial U(Z, S)}{\partial Z} \right|_{Z=\Lambda} = 0 \quad (\text{A.20})$$

$$U(Z = 0, S) = \bar{U} \quad (\text{A.21})$$

The solution for  $U(Z, S)$  can be obtained using Laplace transformation:

$$U(Z, S) = \frac{1}{2\pi i} \int_{\gamma-i\infty}^{\gamma+i\infty} dq e^{qS} \tilde{U}(Z, q) \quad (\text{A.22})$$

where  $\gamma$  is a real number so that the contour path of integration is in the region of convergence of the integrand. For the Laplace transformation

$$\tilde{U}(Z, q) = \int_0^\infty dS e^{-qS} U(Z, S) \quad (\text{A.23})$$

and eq A.18 will give an equation

$$\frac{\partial^2 \tilde{U}(Z, q)}{\partial Z^2} = q \tilde{U}(Z, q) \quad (\text{A.24})$$

Its general solution is  $\tilde{U}(Z, q) = A_q e^{\sqrt{q}Z} + B_q e^{-\sqrt{q}Z}$ . Applying boundary condition (eq A.20), we find  $A_q = B_q e^{-2\sqrt{q}\Lambda}$ , and  $\tilde{U}(Z, q) = B_q \{e^{\sqrt{q}[Z-2\Lambda]} + e^{-\sqrt{q}Z}\}$ . By substituting this result into eq A.21 and taking into account that if the Laplace

original is equal to a Constant, its Laplace transform is equal to  $\text{Const}/q$ . Hence we find,  $B_q = \frac{\bar{U}}{q[1 + e^{-\sqrt{q}2\Lambda}]}$ , and finally

$$\tilde{U}(Z, q) = \bar{U} \frac{\cosh\{(\Lambda - Z)\sqrt{q}\}}{q \cdot \cosh\{\Lambda\sqrt{q}\}} \quad (\text{A.25})$$

The original of this Laplace transform reads<sup>27</sup>

$$\tilde{U}(Z, S) = \bar{U} \left\{ 1 - \frac{2}{\pi} \sum_{n=0}^{\infty} \frac{(-1)^n}{(n + 1/2)} \cos\left[\left(n + \frac{1}{2}\right)\pi\left(1 - \frac{Z}{\Lambda}\right)\right] \exp\left[-\left(n + \frac{1}{2}\right)^2 \pi^2 \frac{S}{\Lambda^2}\right] \right\} \quad (\text{A.26})$$

This is our solution. It is easy to check that it satisfies all the three conditions eqs A.19–A.21. From this solution we can derive any characteristics we are interested in.

### Charge in the Pore

Let us go back to dimensional variables and prepare expressions to calculate the current density and net accumulated charge in the pore if we get  $u(z, t)$  from its dimensionless representation,  $U(Z, S)$ .

If we integrate eq A.1, then we will obtain

$$\begin{aligned} \int_0^L dz \frac{\partial J(z, t)}{\partial z} &= J(L, t) - J(0, t) \\ &= - \int_0^L dz \frac{\partial q(z, t)}{\partial t} \\ &= - \frac{1}{l} \int_0^L dz \frac{\partial \sigma(z, t)}{\partial t} \\ &= \frac{\partial}{\partial t} \left\{ - \frac{1}{l} \int_0^L dz \sigma(z, t) \right\} \\ &= - \frac{1}{l_p} \frac{\partial Q}{\partial t} \end{aligned} \quad (\text{A.27})$$

where

$$Q(t) = l_p \int_0^L dz q(z, t) \frac{\partial q(z, t)}{\partial z} \quad (\text{A.28})$$

is the net charge in the pore accumulated by the time  $t$ . Taking into account that due to the boundary condition of eq A.15, from eq A.27, i.e., from its middle part  $J(0, t) = \frac{1}{l_p} \frac{\partial Q}{\partial t}$ , we get

$$Q(t) = l_p \int_0^t dt' J(0, t') = \Sigma l_p \int_0^t dt' \left. \frac{\partial u(z, t)}{\partial z} \right|_{z=0} \quad (\text{A.29})$$

In dimensional variables (as we prepared our solution in the dimensionless form) this will read:

$$Q(t) = \frac{k_B T}{e} C_0 l_p \int_0^S dS' \left. \frac{\partial U(Z, S')}{\partial Z} \right|_{Z=0} \quad (\text{A.30})$$

Differentiating eq A.26 over  $Z$  and taking this derivative at  $Z = 0$ , we obtain

$$Q = \frac{k_B T}{e} C_0 l_p \Lambda \bar{U} F \left( \frac{\pi^2}{\Lambda^2} S \right) \quad (\text{A.31})$$

$$F(y) \equiv 1 - \frac{2}{\pi^2} \sum_{n=0}^{\infty} \frac{\exp\{-(n + 1/2)^2 y\}}{(n + 1/2)^2} \quad (\text{A.32})$$

In dimensional units eq A.32 will read:

$$Q = Q_{\max} F\left(\frac{\pi^2 l^2 t}{L^2}\right) \quad (\text{A.33})$$

where

$$Q_{\max} = C_0 l l_p \bar{u} \quad (\text{A.34})$$

is the maximal acceptable charge in the pore with the specific capacitance of the double layer  $C_0$ .

Using the obtained solution of eq A.26, we can also derive the equation for the evolution of the charge with the spatial distribution, but this lies beyond the scope of the interests of this paper.

### Limiting Cases

At late times,  $S \rightarrow \infty$ ,  $F(\infty) = 1$ , and  $Q = \frac{k_B T}{e} C_0 l l_p \Lambda \bar{U}$ , which in dimensional units returns

$$Q = Q_{\max} \quad (\text{A.35})$$

This result is correct, as it is the maximal acceptable charge in the pore the specific capacitance of the double of which is  $C_0$ .

At early times,  $S \ll \frac{\Lambda^2}{\pi^2}$ ; in dimensional units, this means  $t \ll \left(\frac{L}{\pi l}\right)^2 \tau$ . This will correspond to small values of  $y$  in eq A.32. Hence, one may evaluate the sum in it replacing it by an integral, i.e., approximating

$$\begin{aligned} F(y) &\approx \frac{2}{\pi^2} \int_0^\infty dx \frac{1 - e^{-yx^2}}{x^2} = \frac{2\sqrt{y}}{\pi^2} \int_0^\infty \frac{1 - e^{-t^2}}{t^2} \\ &= \frac{2}{\pi^{3/2}} \sqrt{y} \end{aligned}$$

(here we have taken into account that  $\frac{2}{\pi^2} \sum_{n=0}^\infty \frac{1}{(n+1/2)^2} = 1$ ).

Hence,  $Q = \frac{k_B T}{e} C_0 l l_p \bar{U} \frac{2}{\pi^{1/2}} \sqrt{S}$ ; in dimensional variables this reads

$$Q = C_0 l l_p \bar{u} \frac{2}{\pi^{1/2}} \sqrt{\frac{t}{\tau}} \quad (\text{A.36})$$

and is a diffusional type of charging.

## ■ APPENDIX B: GENERATING CURRENT WITH PERIODICAL PULSED PRESSURE

Let us consider a problem of generating the electrical current within a transmission line approach for the case when the pulsed pressure is applied. Now let the pressure be  $-P_0$  before the process starts. Then, we assume that the pressure varies in one period of time  $T = \frac{2\pi}{\omega}$  as

$$P(t) = P_0, 0 < t < \frac{\pi}{\omega}; P(t) = -P_0, \frac{\pi}{\omega} < t < \frac{2\pi}{\omega} \quad (\text{B.1})$$

For the next periods, the pressure variation is repeated, so for us it is enough to consider only one period.

Solving the Washburn equation,  $L \frac{dL}{dt} = AP(t)$ ,<sup>8</sup> for the motion of the liquid in the pore leads to the following evolution of the penetration depth

$$L(t) = \sqrt{2AP_0} \sqrt{t}, 0 < t < \frac{\pi}{\omega};$$

$$L(t) = \sqrt{2AP_0} \sqrt{\frac{2\pi}{\omega} - t}, \frac{\pi}{\omega} < t < \frac{2\pi}{\omega} \quad (\text{B.2})$$

This allows us to calculate the evolution of the net charge, using eq 3,

$$Q = \bar{u} C_0 l_p \sqrt{2AP_0} \sqrt{t} \left[ 1 - f\left(\frac{l^2}{2AP_0 \pi \tau}\right) \right], 0 < t < \frac{\pi}{\omega} \quad (\text{B.3})$$

and

$$\begin{aligned} Q &= \bar{u} C_0 l_p \sqrt{2AP_0} \sqrt{\frac{2\pi}{\omega} - t} \\ &\sum_{n=0}^{\infty} \frac{1}{\left(n + \frac{1}{2}\right)^2} \times \left[ 1 - e^{-\left(n + \frac{1}{2}\right)^2 \pi^2 l^2 t / 2AP_0 \left(\frac{2\pi}{\omega} - t\right) \tau} \right] \end{aligned} \quad (\text{B.4})$$

Then, we can easily calculate the generated current. In the first half of the period, it can be shown that

$$J(t) = \bar{u} C_0 l_p \frac{\sqrt{2AP_0}}{2\sqrt{t}} \left[ 1 - f\left(\frac{l^2}{2AP_0 \pi \tau}\right) \right] \quad (\text{B.5})$$

In the next step, following the procedure described in the main text, we can estimate the generated power density considering only one-half of the period. It can be shown that

$$\langle J \rangle = \frac{\varepsilon}{\pi r^2} \frac{\omega}{\pi} Q \left( \frac{\pi}{\omega} \right) \quad (\text{B.6})$$

which leads to the following expression for the “short-circuit” power density:

$$W = \frac{\varepsilon}{l} \sqrt{\frac{2}{\pi}} C_0 \bar{u}^2 \sqrt{AP_0 \omega} \left[ 1 - f\left(\frac{l^2}{2AP_0 \pi \tau}\right) \right] \quad (\text{B.7})$$

In the limit when the ion migration time is very short, the power density is equal to

$$W = \frac{\varepsilon}{l} \sqrt{\frac{2}{\pi}} C_0 \bar{u}^2 \sqrt{AP_0 \omega} \quad (\text{B.8})$$

One can see from eq B.7 that the power density depends on the frequency as  $\sim \sqrt{\omega}$ , i.e., in the same way as for the case with sinusoidal variation in the pressure described in the main text. Similarly, we can estimate the dependence on the maximal exerted pressure. At small pressures the power density behaves as described in eq B.8, while for larger pressure it saturates to the value

$$W = \frac{2\varepsilon C_0 \bar{u}^2}{\pi} \sqrt{\frac{\omega}{\tau}} \quad (\text{B.9})$$

Thus, the current generation for the pulsed staircase variation of the pressure is qualitatively similar to the case of the sinusoidal variation considered in detail in the main text. The only difference is in the magnitude of the corresponding quantities.

## ■ APPENDIX C: WHEN WE CAN NEGLECT THE OHMIC LOAD IN THE CALCULATION OF GENERATED CURRENT

For the purpose of the estimate that we will obtain below, let us neglect all the effects of ion migration limitations, the main subject of the present paper. In that case, varying the capacitance  $C$  with time,  $t$ , at a constant bias voltage  $\bar{u}$ , we provide with no delay the charge stored in the capacitor. Ideally, the time dependence of charge should reproduce the time dependence of the capacitance

$$Q(t) = C(t)\bar{u} \quad (\text{C.1})$$

However, eq C.1 does not take into account Ohm's voltage drop in the circuit. Taking the latter into account, instead of eq C.1, we should write

$$Q(t) = C(t)V_c(t) \quad (\text{C.2})$$

Here  $V_c(t)$  is the voltage drop across the capacitor, which is only a part of the total voltage drop and it will be time dependent, because

$$V_c(t) = \bar{u} - V_{\text{Ohm}}(t) \quad (\text{C.3})$$

with

$$V_{\text{Ohm}}(t) = RI(t) = R \frac{dQ(t)}{dt} \quad (\text{C.4})$$

where  $R$  is the circuit resistance, dominated by the load.

Combining eqs C.2–C.4, we obtain a linear differential equation on  $Q(t)$ :

$$R \frac{dQ}{dt} + \frac{Q}{C(t)} - \bar{u} = 0 \quad (\text{C.5})$$

Its solution could be investigated for a given form of  $C(t)$  (for example, see ref 6). However, we will not be doing it here and instead estimate the importance of the difference between eq C.5 and the simplified eq C.1. The difference is unimportant if the first term in eq C.5 can be neglected with respect to the two other terms. The estimate can be obtained by iteration, substituting in the first term the "zero-order" approximation,  $Q(t) \approx C(t)\bar{u}$  and thus obtaining the requirement,  $\left| R \frac{dC}{dt} \bar{u} \right| \ll |\bar{u}|$ , i.e.,

$$R \left| \frac{dC}{dt} \right| \ll 1 \quad (\text{C.6})$$

If  $C(t)$  is some kind of periodic function of time with amplitude  $C_0$  and frequency  $\omega$  (as in ref 6), then eq C.6 will give

$$\omega \ll 1/RC_0 \quad (\text{C.7})$$

Consider our typical 1 s period; thus,  $\omega = 2\pi \text{ s}^{-1}$ . For a current generated just by one pore, this criterion will of course be satisfied. Indeed, even if we take a load with  $R = 10 \text{ k}\Omega$  and  $C_0 = 0.1 \text{ F/m}^2(2\pi rL) = 0.1 \text{ F/m}^2(2\pi \times 10^{-6} \text{ m})(2 \times 10^{-3} \text{ m}) = 1.26 \times 10^{-9} \text{ F}$ , we get a requirement of  $\omega \ll 10^5 \text{ s}^{-1}$ . However, this is only for one pore! The number of such pores in a  $50 \text{ cm}^2$  sole at 10% porosity will be  $1.6 \times 10^8$ ; hence, the capacitance will be that many times larger, ending up with the constraint  $\omega \ll 10^{-3} \text{ s}^{-1}$ . Thus, if we want to describe the current generated by the whole shoe, neglecting the circuit resistance, then we cannot allow the resistance to be larger than  $\sim 1 \text{ }\Omega$ . Of course, if we reduce the area from which we collect the current, say to  $1 \text{ cm}^2$ , we could afford 50 times larger

resistance for the current calculation to remain valid, whereas for a  $1 \text{ mm}^2$  sensor it could be  $5 \text{ k}\Omega$

When criterion eq C.9 is fulfilled and the load can be neglected in the calculation of the current, the power accumulated in the load would, of course, depend on the load and will be equal to  $\langle I(t)^2 \rangle R$ .

Similar analysis which accounts for ion transport limitations would be much more cumbersome and unlikely possible in analytical terms, but since the transmission line charging slows down variation of charge, the effect of the first term in eq C.5 would be smaller than in the adiabatic approximation.

## ■ AUTHOR INFORMATION

### Corresponding Author

\*E-mail: a.kornyshev@imperial.ac.uk.

### ORCID

Alexei A. Kornyshev: 0000-0002-3157-8791

Anatoly B. Kolomeisky: 0000-0001-5677-6690

### Notes

The authors declare no competing financial interest.

## ■ ACKNOWLEDGMENTS

We are thankful to Tom Krupenkin and Gunnar Pruessner for useful discussions. We acknowledge Engineering and Physical Sciences Undergraduate Research Opportunity (UROP) vacation bursary to R.M.T. which has made possible her work on the project.

## ■ REFERENCES

- (1) Mirfakhrai, T.; Madden, J. D. W.; Baughman, R. H. Polymer Artificial Muscles. *Mater. Today* **2007**, *10*, 30–38.
- (2) Lee, A. A.; Colby, R.; Kornyshev, A. A. Electroactuation with Single Charge Carrier Ionomers: The Roles of Electrostatic Pressure and Steric Strain. *Soft Matter* **2013**, *9*, 3767–3776.
- (3) Fink, J. K. *Polymeric Sensors and Actuators*; Wiley-Scrivener Publishing: Salem, MA, 2013.
- (4) Nie, B.; Li, R.; Brandt, J. D.; Pan, T. Ionotropic Microdroplet Array for Flexible Ultrasensitive Tactile Sensing. *Lab Chip* **2014**, *14*, 1107–16.
- (5) Krupenkin, T. N. Method and Apparatus for Energy Harvesting using Microfluidics. U.S. Patent 8,053,914 B1, November 8, 2011.
- (6) Krupenkin, T.; Taylor, J. A. Reverse Electrowetting as a New Approach to High-Power Energy Harvesting. *Nat. Commun.* **2011**, *2*, 448.
- (7) Hsu, T.-H.; Manakasettharn, S.; Taylor, J. A.; Krupenkin, T. Bubbler: A Novel Ultra-High Power Density Energy Harvesting Method Based on Reverse Electrowetting. *Sci. Rep.* **2015**, *5*, 16537.
- (8) Kolomeisky, A. B.; Kornyshev, A. A. Current-Generating 'Double Layer Shoe' with a Porous Sole. *J. Phys.: Condens. Matter* **2016**, *28* (46), 464009.
- (9) Quere, D. Wetting and Roughness. *Annu. Rev. Mater. Res.* **2008**, *38*, 71–98.
- (10) Washburn, E. W. The Dynamics of Capillary Flow. *Phys. Rev.* **1921**, *17*, 273–283.
- (11) Bear, J. *Dynamics of Fluids in Porous Media*; Dover: New York, 1988.
- (12) Ralston, J.; Popescu, M.; Sedev, R. Dynamics of Wetting from Experimental Point of View. *Annu. Rev. Mater. Res.* **2008**, *38*, 23–43.
- (13) Joly, L. Capillary Filing with Giant Liquid/Solid Slip: Dynamics of Water Uptake by Carbon Nanotubes. *J. Chem. Phys.* **2011**, *135*, 214705.
- (14) Biesheuvel, P. M.; Bazant, M. Nonlinear Dynamics of Capacitive Charging and Desalination by Porous Electrodes. *Phys. Rev.* **2010**, *81*, 031502.

- (15) Biesheuvel, P. M.; van Limpt, B.; van der Wal, A. Dynamic Adsorption/Desorption Process Model for Capacitive Deionization. *J. Phys. Chem. C* **2009**, *113*, 5636–5640.
- (16) Burheim, O. S.; Liu, F.; Sales, B. B.; Schaetzle, O.; Buisman, C. J. N.; Hamelers, H. V. M. Faster Time Response by the Use of Wire Electrodes in Capacitive Salinity Gradient Energy Systems. *J. Phys. Chem. C* **2012**, *116*, 19203–19210.
- (17) Ahualli, S.; Fernandez, M. M.; Iglesias, G.; Jiménez, M. L.; Liu, F.; Wagterveld; Delgado, A. V. Effect of Solution Composition on the Energy Production by Capacitive Mixing in Membrane-Electrode Assembly. *J. Phys. Chem. C* **2014**, *118*, 15590–15599.
- (18) Porada, S.; Zhao, R.; Van der Wal, A.; Presser, V.; Biesheuvel, P. M. Review of Science and Technology of Water Desalination by Capacitive Deionization. *Prog. Mater. Sci.* **2013**, *58*, 1388–1442.
- (19) Washburn, E. W. The Dynamics of Capillary Flow. *Phys. Rev.* **1921**, *17*, 273–83.
- (20) Cannon, J. R. *The One-Dimensional Heat Transfer (Encyclopaedia of Mathematics and Its Applications)*; Addison-Wesley/Cambridge University Press: Reading, U.K., 1984.
- (21) Kornyshev, A. A. The Simplest Model of Charge Storage in Single File Metallic Nanopores. *Faraday Discuss.* **2013**, *164*, 117–133.
- (22) Kolomeisky, A. B.; Kornyshev, A. A. Corrigendum: Current-generating ‘double layer shoe’ with a porous sole. *J. Phys.: Condens. Matter* **2017**, *29* (4), 049501.
- (23) Szymczyk, A.; Labbez, C.; Fievet, P.; Vidonne, A.; Foissy, A.; Pagetti, J. Contribution of Convection, Diffusion and Migration to Electrolyte Transport through Nanofiltration Membranes. *Adv. Colloid Interface Sci.* **2003**, *103*, 77–94.
- (24) Hunter, R. J. *Foundations of Colloid Science*, 2nd ed.; Oxford University Press: Oxford, U.K., 2001.
- (25) Ulaby, F. T. *Fundamentals of Applied Electromagnetics*; Prentice Hall: Boston, MA, 2004.
- (26) de Levie, R. On Porous Electrodes in Electrolyte Solutions. *Electrochim. Acta* **1963**, *8*, 751–780.
- (27) Bateman, H.; Erdélyi, A. *Tables of integral transforms 1*; McGraw-Hill: New York, 1954.